

63-3-3

NWRF15 0163 072

*A Case Study of  
Radioactive Fallout*

403 276

by

Elmar R. Reiter

Prepared Under Contract No. N 189(188)55120A  
With U. S. Weather Research Facility, Norfolk, Va.

Technical Paper No. 42  
Department of Atmospheric Science  
Colorado State University  
Fort Collins, Colorado



January 1963

CER63ERR7

QUALIFIED REQUESTERS MAY OBTAIN COPIES OF THIS REPORT DIRECT FROM ASTIA

ORIGINAL BY ROUTE  
AS AD NO. 403276

**A CASE STUDY OF RADIOACTIVE FALLOUT<sup>1</sup>**

by:

**Elmar R. Reiter**

<sup>1</sup>The research reported in this paper has been conducted under Contract N 189(188)55120 A with U. S. Navy Weather Research Facility.

<sup>2</sup>Project Leader, Associate Professor.

## A CASE STUDY OF RADIOACTIVE FALLOUT

### Abstract:

During September 1961 a series of balloon ascents made from Flin Flon, Canada, carrying scintillation counters sensitive to gamma radiation, revealed the existence of shallow stable atmospheric layers carrying radioactive debris, presumably from the Russian test series during the same month.

The debris layers encountered on September 14 and 15 have been studied in particular. The debris detected over Flin Flon on September 14, 2221 GCT, at 650 mb had undergone strong sinking motion. One may conclude that it came out of the stratosphere shortly prior to September 13, 12 GCT, entering the troposphere through the stable layer underneath the jet core, sometimes referred to as "jet-stream front".

Beginning with September 17 a distinct area of radioactive fallout begins to appear at the surface over the eastern United States. Some of this debris seems to be identical with the one detected over Flin Flon, and it apparently was transported by the same jet stream. Part of the fallout is associated with a small collapsing cold dome travelling ahead of this jet stream.

## INTRODUCTION

During the period September 14 to October 1, 1961 nine high-altitude constant-level balloons were released from Flin Flon, Canada, for the purpose of studying x-ray fluxes associated with electron precipitation during magnetic storms and auroras. Seven of these flights traversed thin layers of air which emitted gamma radiation at a rate significantly above that which could be attributed to cosmic radiation effects (Anderson, 1962). Because of the shallowness of these layers and their occurrence at relatively low levels in the atmosphere, it is obvious that their radiation could not have originated outside the atmosphere. We are forced to conclude that the gamma radiation emanates from suspended radioactive debris, which is found to be concentrated in rather thin layers. The following table contains some of the results from these balloon meas-

urements.

In all these cases the radioactive debris was found in stable layers. This conforms to results obtained from a recent investigation by Staley (1962), whose radioactivity data were obtained from aircraft sampling flights. Therefore, they do not give a continuous radiation-altitude profile, and do not reveal the astounding shallowness of debris layers evident from Anderson's measurements.

From the cases presented in Table I, those of September 14 and 15 will be described in detail because they occurred low enough in the atmosphere to permit the utilization of Canadian wind data for the construction of isentropic trajectories.

Table I. Specific Activities of Radioactive Debris over Flin Flon, Canada (Anderson, 1962)  
September 1961

Date	Time of Observation UT	Atmospheric Pressure at Center of Cloud	Atmospheric Density at Center of Cloud	Absorption Coefficient for 0.8 Mev Gammas	Length in Which Gamma Intensity Falls by 1/e (Theoret. Values)	Observed Vertical Distance Over which Gamma Envelope of Cloud Falls by 1/e	Specific Activity Microcuries Per Cubic Meter
14	2221	650 mb	$8.8 \times 10^{-4} \frac{g}{cm^3}$	$2.6 \times 10^{-5} cm^{-1}$	167 meters	425	0.19
15	1236	758	9.75	2.9	145	335	0.014
18	0024	205	3.3	1.0	435	1830	0.085
25	0225	210	2.65	0.8	540	-	0.004
27	2352*	175	2.40	0.72	595	3370	0.014
	2358	125					0.010
28	1453	97	1.55	0.47	925	3070	0.11
30	0230	205	2.6	0.8	-	-	$4 \times 10^{-4}$

\* This cloud has two separate peaks.

**THE WEATHER SITUATION, SEPTEMBER 13 to 21, 1961**

In Figs. 1 and 2 the 500 mb and surface weather maps of 1200 GCT are presented for the period September 13 through 21, 1961. The beginning of this period was characterized by a pronounced ridge in the upper flow pattern over the western parts of the continent. A trough over the central United States contains a small cut-off low on the 500-mb surface over North Dakota on September 13. This pocket of cold air is rapidly collapsing on the subsequent days, as will be evident from the isentropic analyses presented farther below. The low level divergence and sinking motion within this cold-air pool is in qualitative agreement with the surface high-pressure system which on September 13 is located underneath the cut-off low over the north central United States, and which moves over the eastern United States by September 20.

Towards the end of the period of investigation the weather over the eastern United States is increasingly influenced by hurricane "Esther", which starts moving northward along the Atlantic Seaboard on September 20.

On September 13 a jet stream appears over

the Northwestern Territory (Fig. 3). Sachs Harbor (051) reports winds blowing with 59 m/sec from 311° on September 13, 1200 GCT at the 250-mb level. Mould Bay (072) reports 30 m/sec from 325° at the same time and level, and Inuvik (957) only 13 m/sec from 220°. It appears therefore that the jet axis lies very close to the station Sachs Harbor, a fact which will be stressed again farther below. A shear line which extends from North Dakota to Hudson Bay coincides with the position of the upper trough in Fig. 1. Sinking motion, which seems to characterize such shear lines (Hsieh, 1950) causes the collapse of the cold dome mentioned above.

Between September 14 and 16 this jet stream proceeds towards the Hudson Bay and Labrador region where it merges with a southwesterly jet which had previously dominated the upper-flow regime over the central United States (Fig. 1). During the next two days the main belt of the westerlies seems to be confined to Canada. From September 19 to the end of the period under consideration a new trough approaching from the west causes the upper flow over the central United States to back to a southwesterly direction.

Fig. 1 500-mb topographies (200-ft. contour interval), for 1200 GCT and dates as indicated on maps.

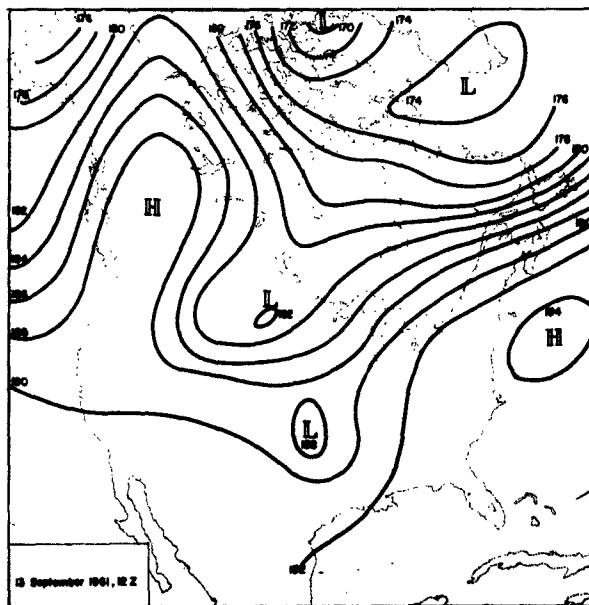


Fig. 1 continued.

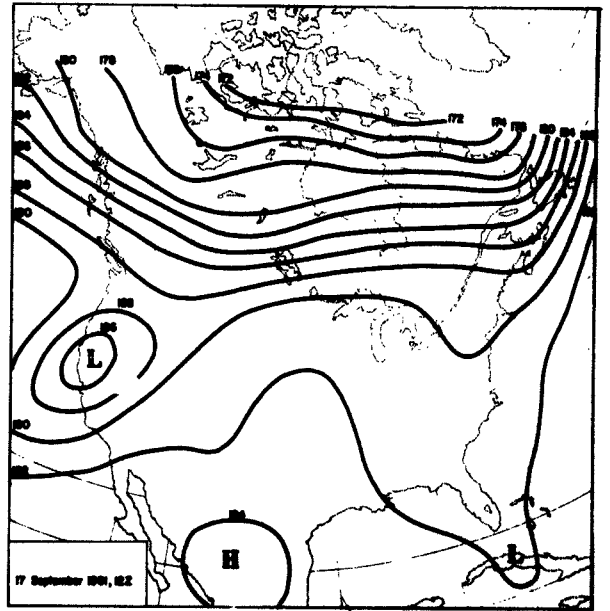
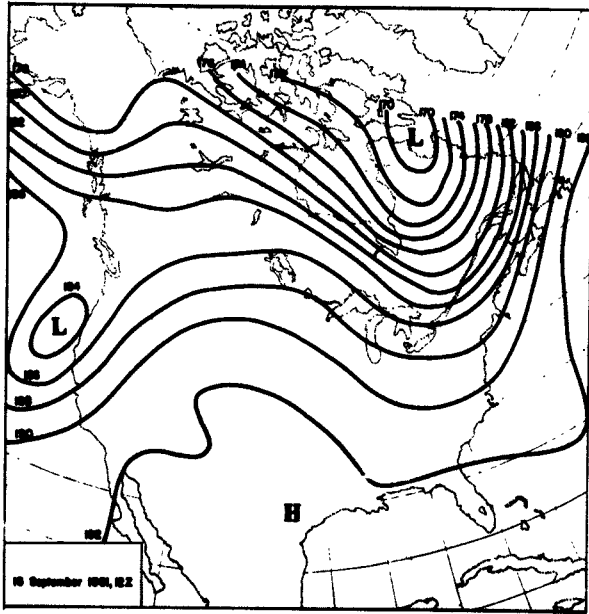
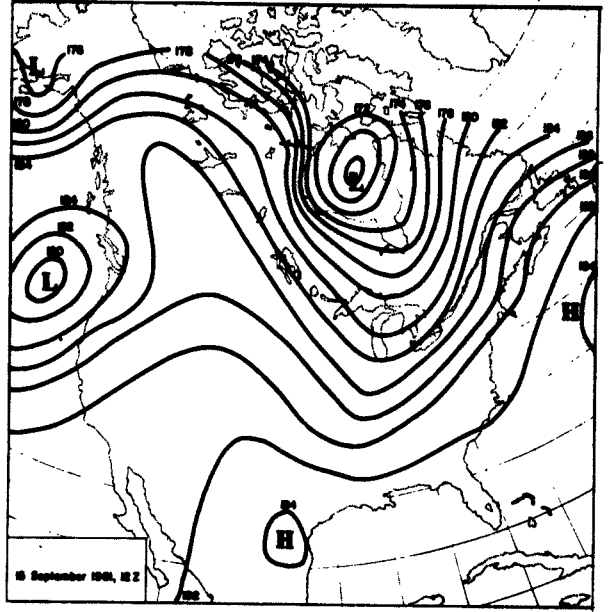
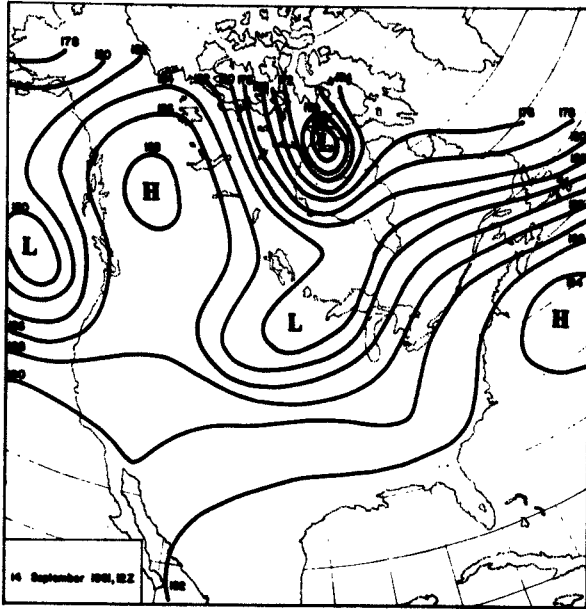
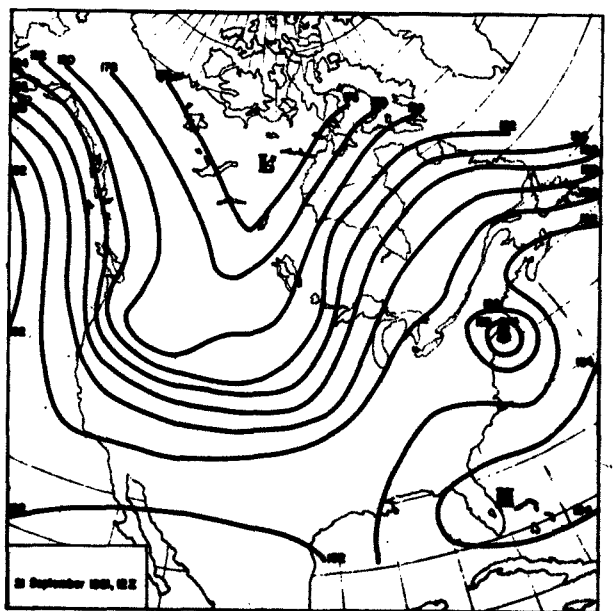
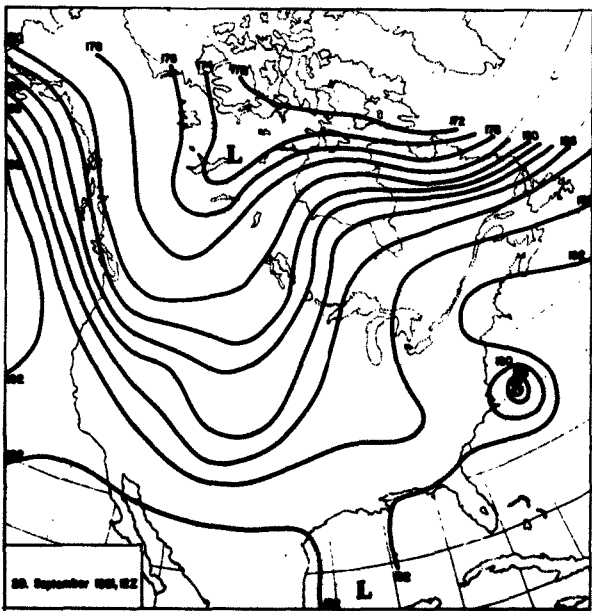
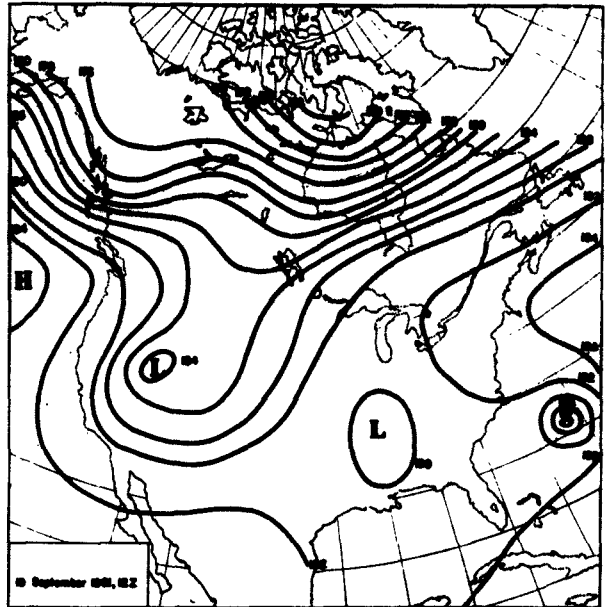
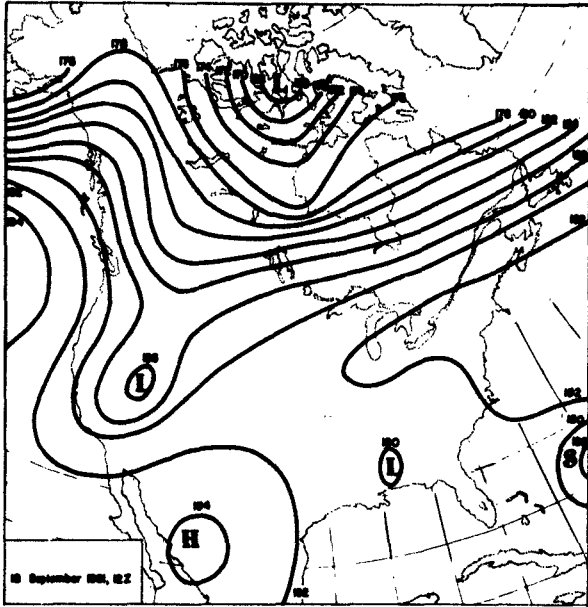


Fig. 1 continued.



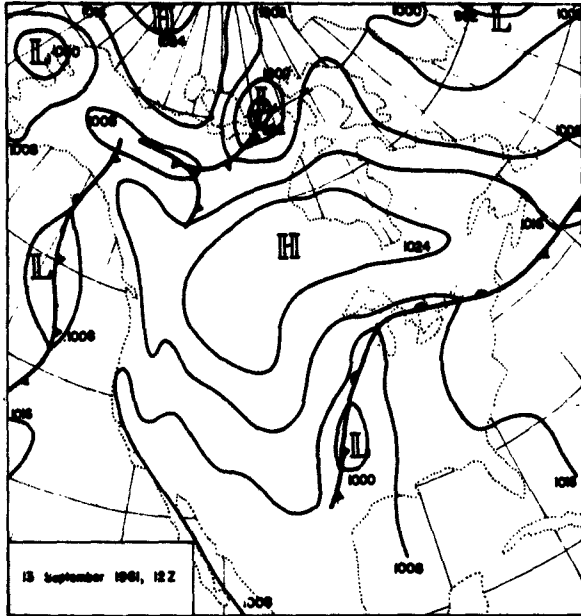


Fig. 2 Surface pressure distribution (8-mb interval of isobars) for 1200 GCT and dates as indicated on maps.

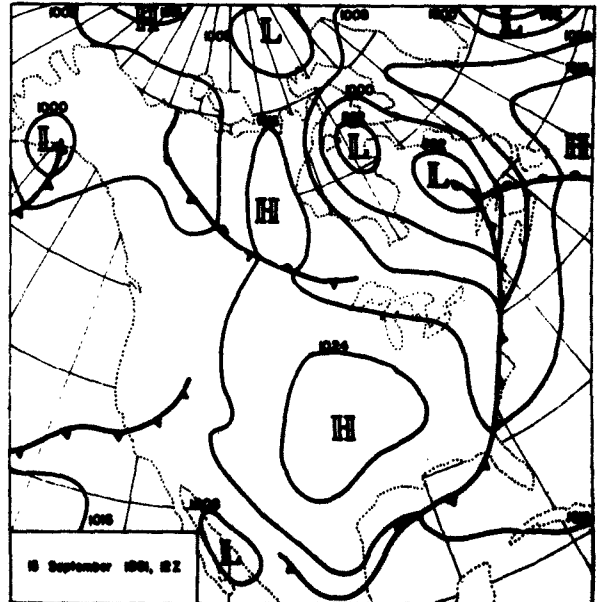
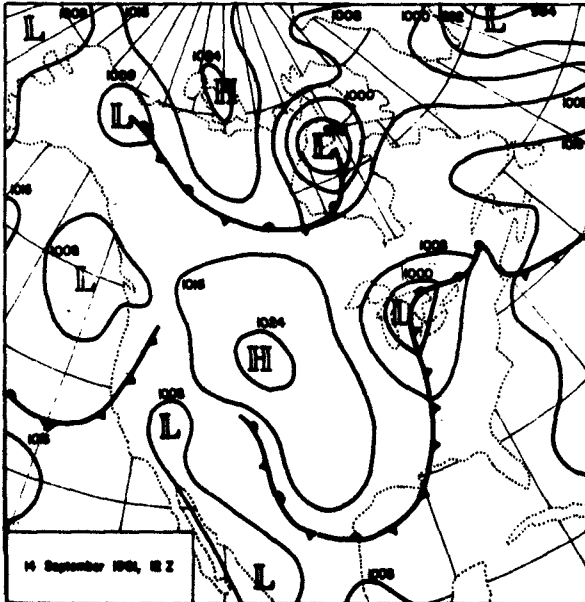


Fig. 2 continued.

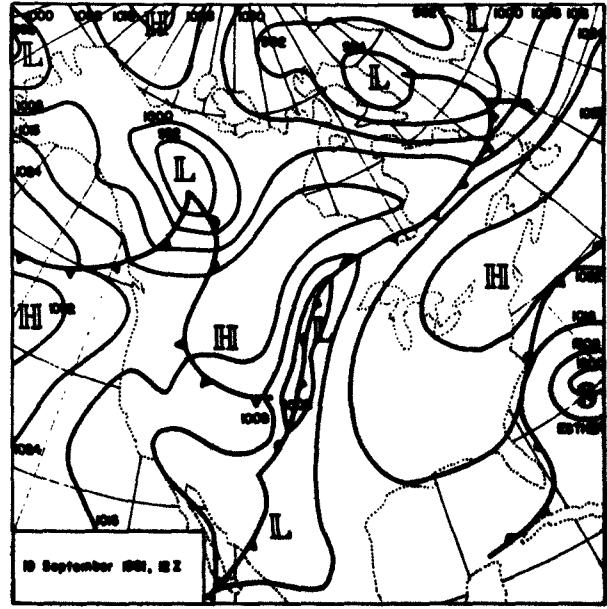
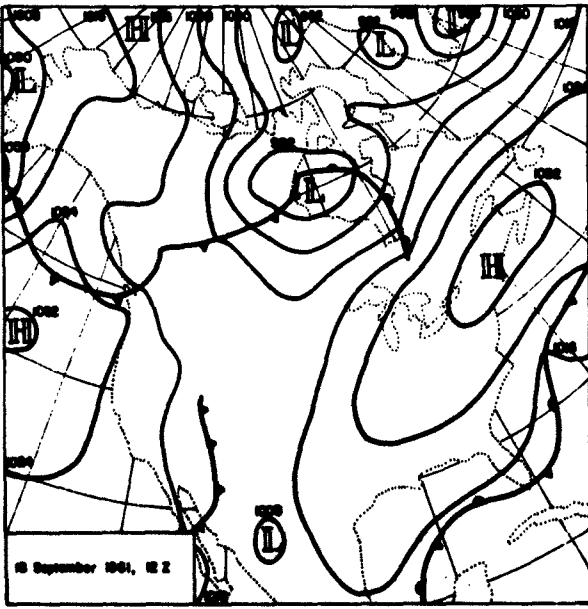
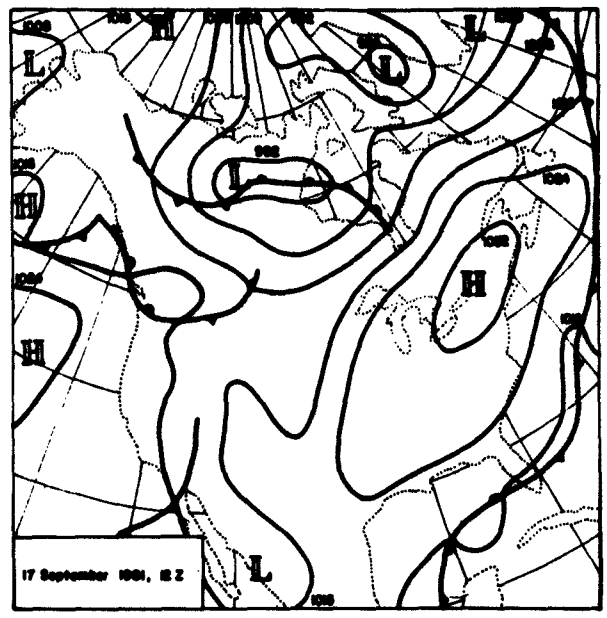
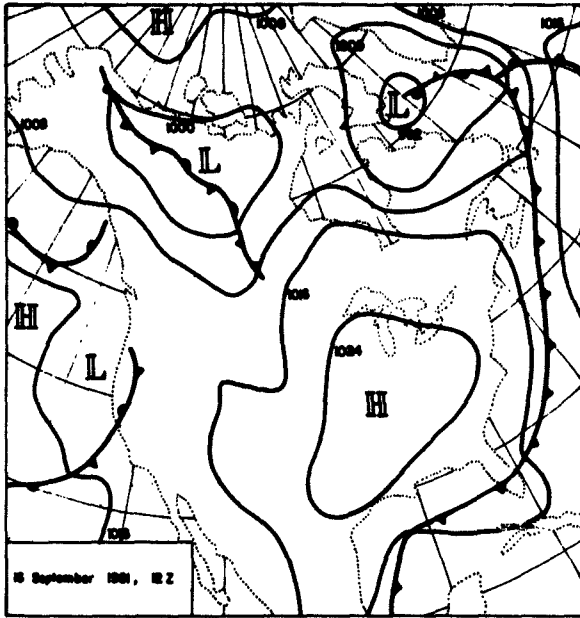


Fig. 2 continued.

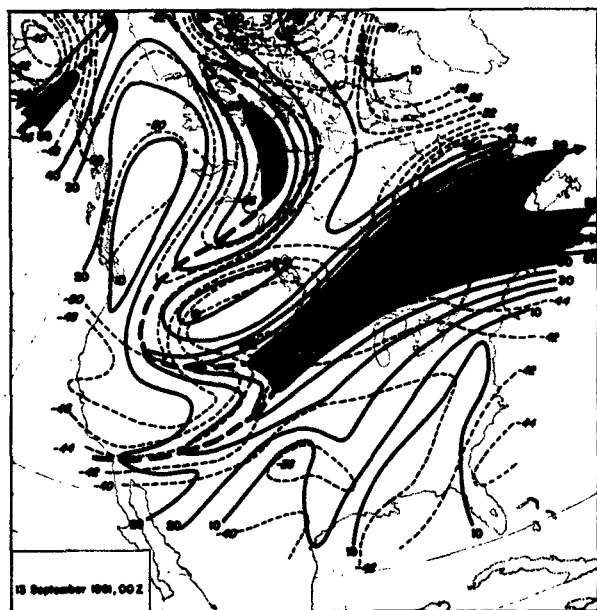
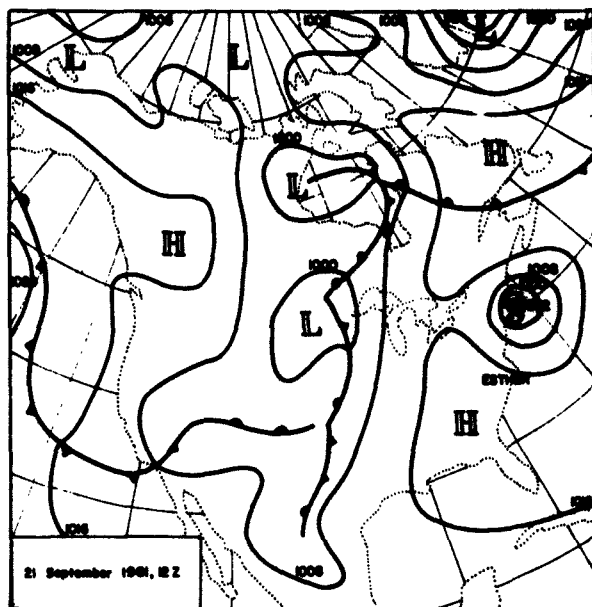
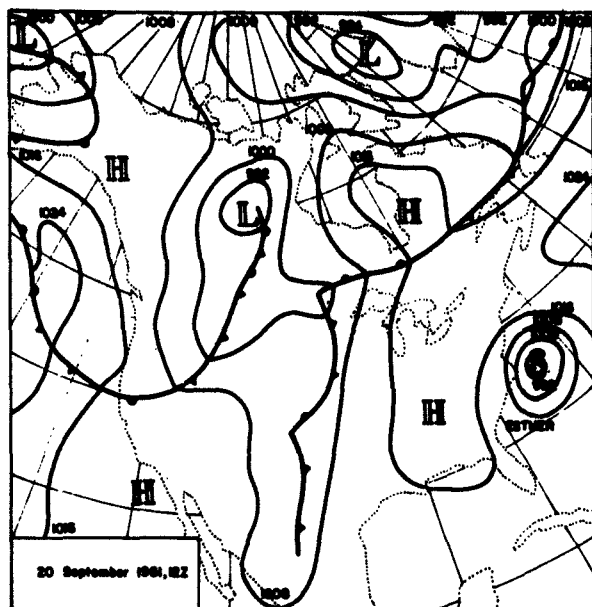


Fig. 3 250-mb isotachs (full lines, vertical numbers, m/sec, areas with speeds > 50 m/sec are shaded) and isotherms (thin dashed lines, slant numbers  $^{\circ}\text{C}$ ) for dates and observation times as indicated on maps. Heavy dashed lines indicate jet axes.

Fig. 3 continued.

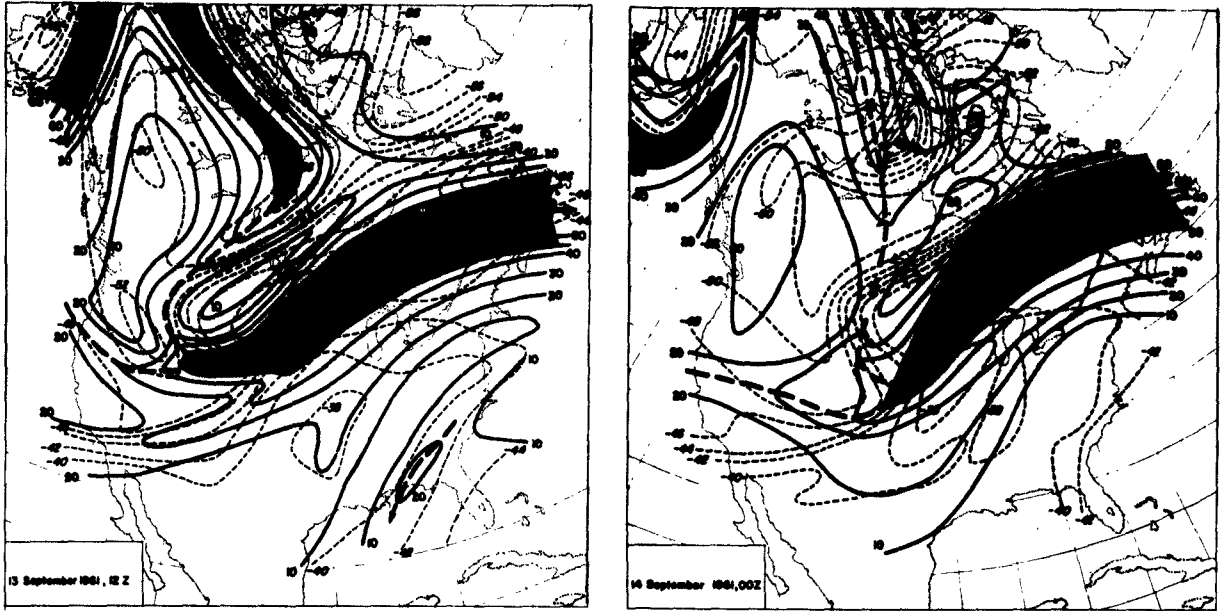
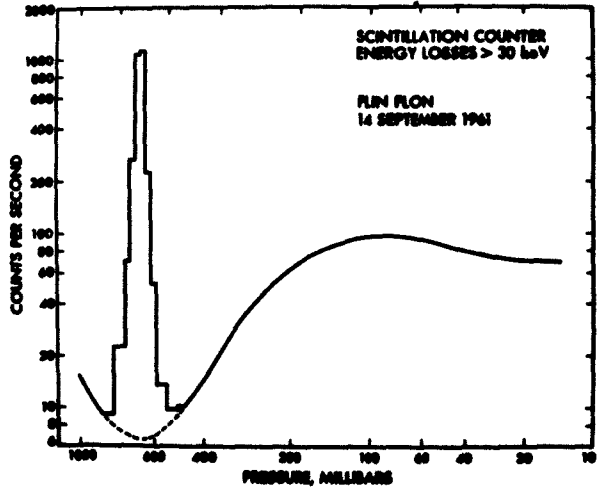


Fig. 4 Scintillation counts per second (ordinate) as a function of pressure (mb) for balloon flight of 14 September 1961, 22 GCT, released from Flin Flon, Canada.



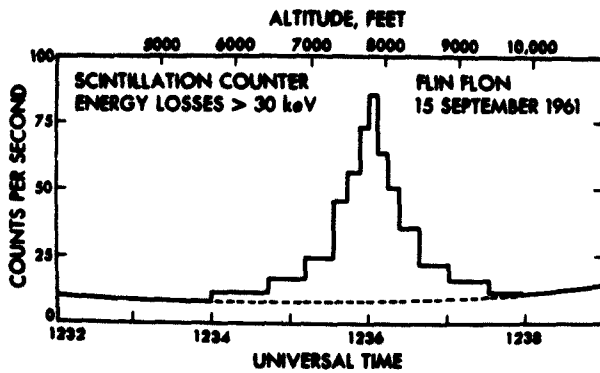


Fig. 5 Scintillation counts per second (ordinate) as a function of time (GCT), for balloon flight of 15 September 1961, released from Flin Flon, Canada.

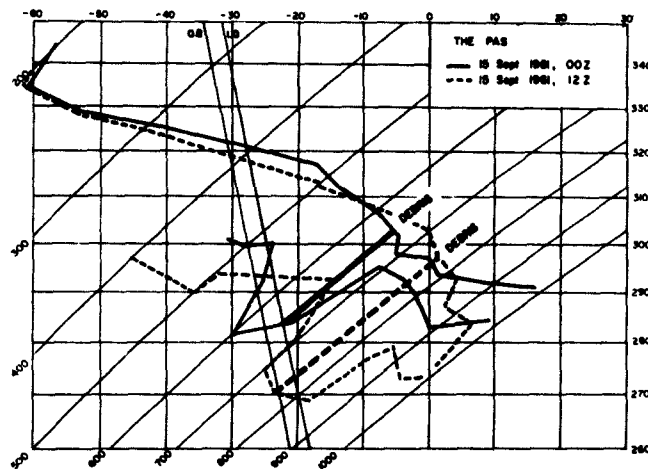


Fig. 6 Temperature and dew point temperature soundings of The Pas(867), 15 September 1961, 0000 and 1200 GCT, plotted on a tephigram. Horizontal coordinate: temperature; vertical coordinate: potential temperature; curved lines from lower left to upper right: pressure; lines labeled 0.8 and 1.0 are lines of constant mixing ratio. The pressure levels at which the debris clouds were encountered are marked by a heavy solid, respectively dashed line.

#### THE DEBRIS CLOUDS OF SEPTEMBER 14 and 15, 1961

Figs. 4 and 5 show the counts per second obtained from the scintillation detector on September 14 and 15, 1961 over Flin Flon. The dashed portions in these two diagrams indicate the "normal" radiation profile in the absence of radioactive debris. Especially the debris cloud encountered at 2221 GCT, September 14, is very pronounced and shows a counting rate almost three orders of magnitude higher than normal.

Fig. 6 contains the soundings of The Pas (867), located approximately 100 miles to the south

of Flin Flon. The dew point temperatures have been re-computed from the relative humidity values given in the "Northern Hemisphere Data Tabulations, Daily Bulletin". In both instances the debris clouds are confined in a shallow, stable, and very dry layer. According to previous findings (Staley, 1960; Danielsen, 1959, 1961; Danielsen and Reiter, 1960; Reiter, 1961a) such layers usually maintain their identity while advected over large distances. They constitute a characteristic feature of the atmospheric meso- and microstructure, as is also evident from detailed flight measurements (Reiter, 1961b; Reiter, 1962; Reiter, Lang et al., 1961).

It has been pointed out by Reed and Danielsen (1959), that most of the air-mass exchange between stratosphere and troposphere seems to occur through the gap between polar and subtropical tropopause in the vicinity of a jet stream. The air within this stable zone, which sometimes has been referred to as "jet-stream front" (Endlich et al., 1957), is characterized by high values of potential vorticity of the same order of magnitude as one finds in the stratosphere immediately to the north and above the jet core (see also Reiter, 1961c), suggesting the stratospheric origin of air contained in this layer. Furthermore, this air is relatively dry and has a high ozone content (Murgatroyd, 1959; see also Reiter, 1961a), indicative of the sinking motion to which it is subjected.

Under the assumption that atomic debris has been injected into the stratosphere by the Russian test series of autumn 1961, we might surmise that the radioactive layers encountered in the lower troposphere on September 14 and 15 over Flin Flon, owing to their extreme dryness, have come out of the stratosphere and have undergone strong sinking motions.

Fig. 7 shows Montgomery stream-function analyses of the 303°K isentropic surface, together

with the isobars of this surface for the period September 13, 1961, 0000 GCT to September 15, 0000 GCT, when radioactive debris was encountered in this potential-temperature surface over Flin Flon (Fig. 6).

The isentropic stream-function values

$$M = c_p T_\theta + g z_\theta \quad (1)$$

have been computed from the expression

$$M = c_p \theta \left( \frac{p_\theta}{1000} \right)^{\frac{R}{c_p}} + g z_p + R \bar{T} \ln \frac{p}{p_\theta} \quad (2)$$

where  $\theta$  is the potential temperature of the particular isentropic surface under consideration;  $p_\theta$  is the pressure at this surface;  $z_p$  is the height of the standard isobaric surface closest to this isentropic surface;  $\bar{T}$  is the mean temperature between standard isobaric and isentropic surface. The following values have been assumed for the various constants in equation (2):

Fig. 7 Montgomery stream function ( $10^7 \text{ erg g}^{-1}$ , heavy solid lines, vertical numbers and isobars (mb, thin dashed lines, slant numbers) for isentropic surface 303°K and for dates and observation times as indicated on charts. Progressively denser shading is used for wind speeds >15, 25 and 35 knots. Shading with heavy lines (15 September, 00 GCT) marks intersection of this isentropic surface with the ground.

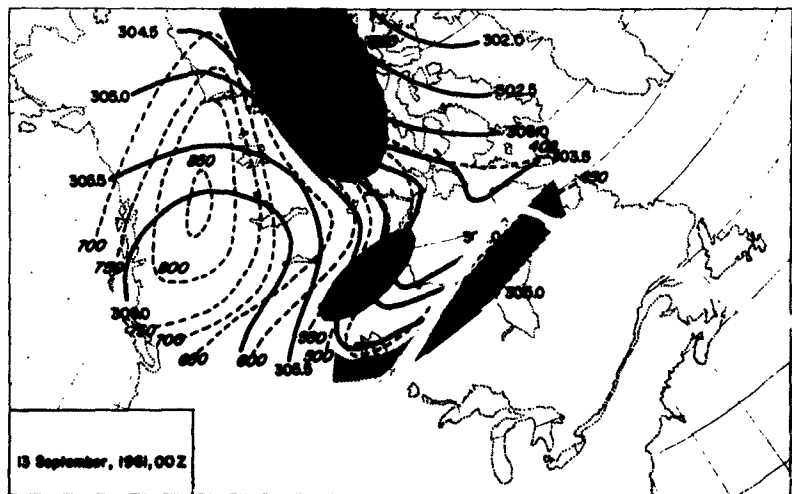


Fig. 7 continued.

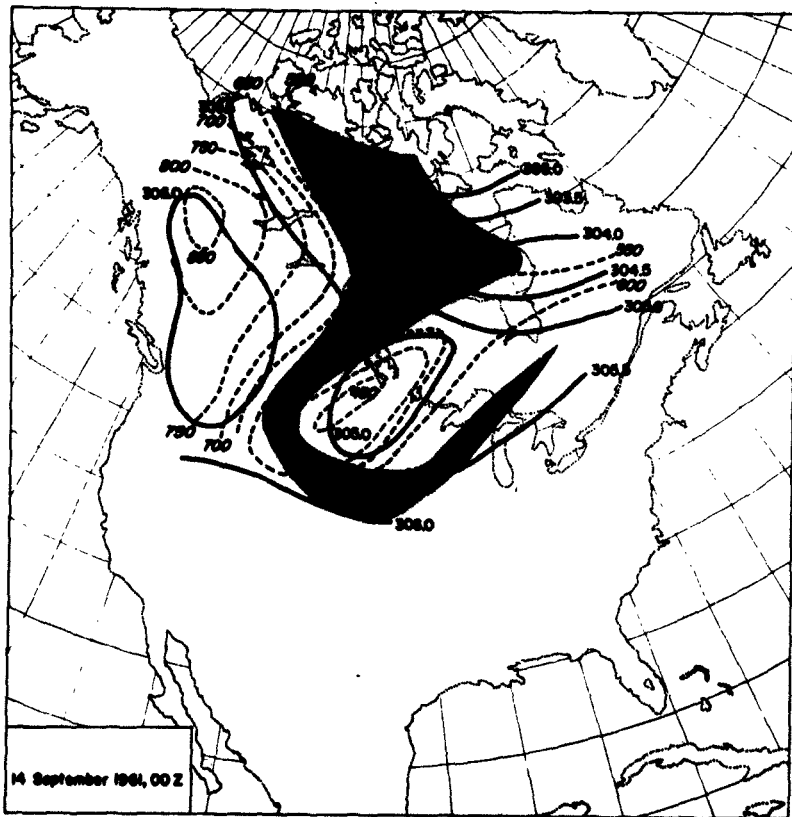
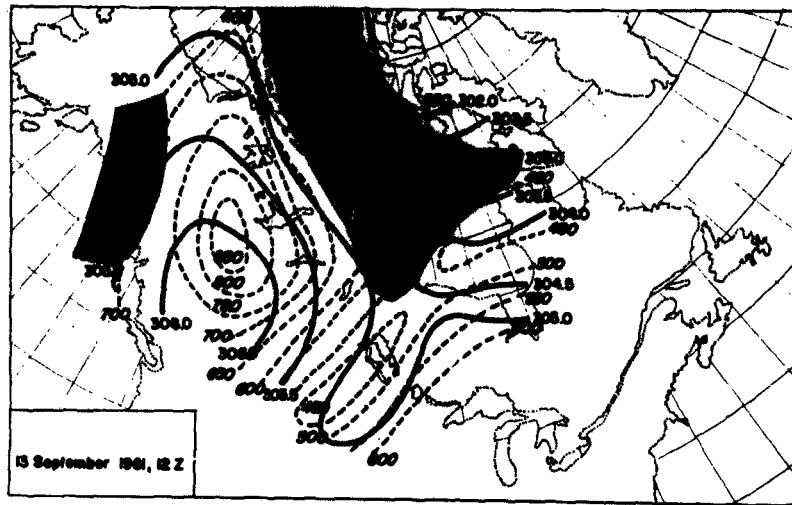
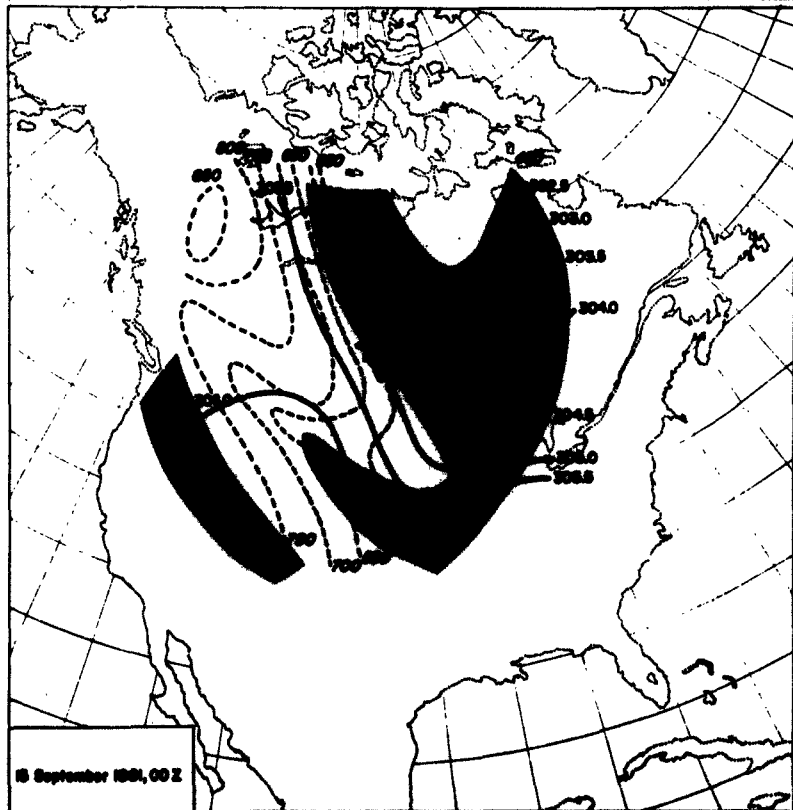
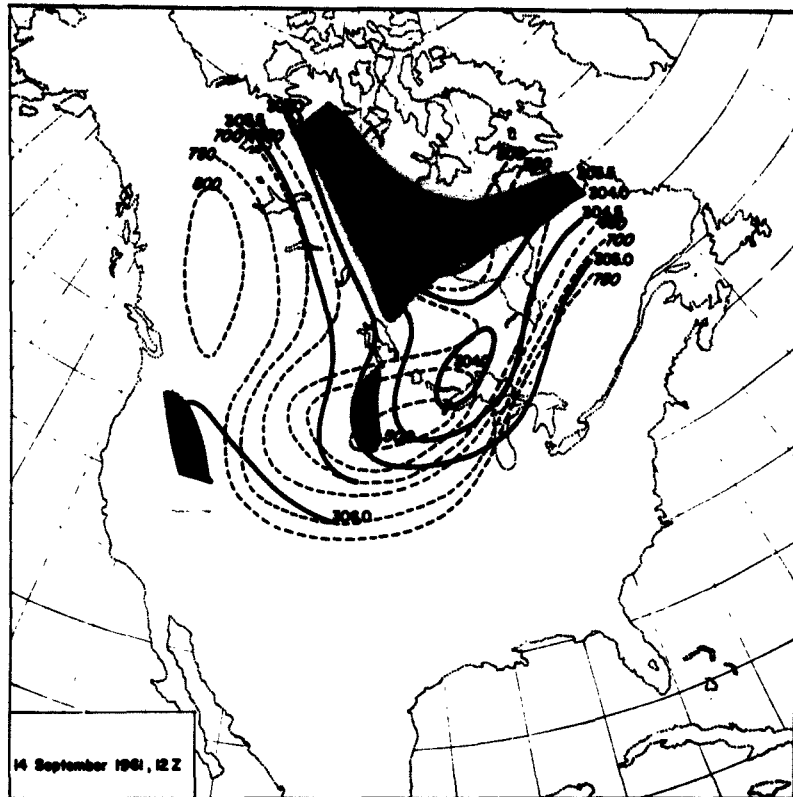


Fig. 7 continued.



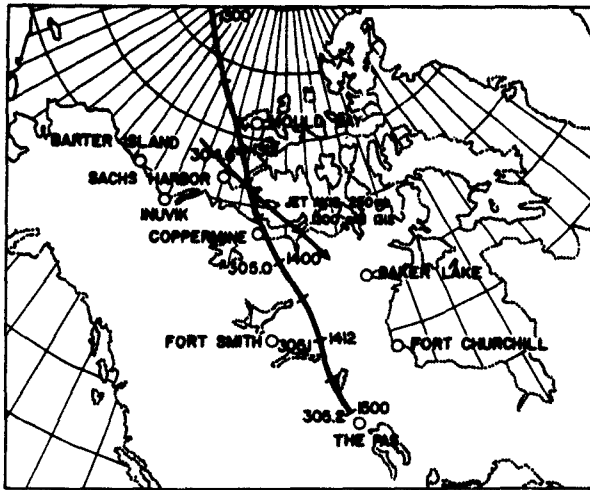


Fig. 8 Isentropic trajectory along the  $303^{\circ}\text{K}$  surface, September 13, 1961, 00 GCT to September 15, 00 GCT. Numbers to the left of the trajectory give the stream-function value ( $10^7 \text{ erg g}^{-1}$ ), to the right the observation time.

$$g = 980.6 \text{ cm sec}^{-2}$$

$$c_p = 1.0046 \times 10^7 \text{ erg g}^{-1} \text{ deg}^{-1}$$

$$c_v = 0.7176 \times 10^7 \text{ erg g}^{-1} \text{ deg}^{-1}$$

$$R = 2.8704 \times 10^6 \text{ erg g}^{-1} \text{ deg}^{-1}$$

With these the stream function may be computed from

$$M = 1.4005 \times 10^6 \theta \times p_{\theta}^{0.2857} + 9.806 \times 10^4 \times z_p + 2.8704 \times 10^6 \frac{p}{T} \times \log_{10} \frac{p_p}{p_{\theta}} \quad (3)$$

Fig. 8 contains the isentropic trajectory of an air particle, which travels in the  $303^{\circ}\text{K}$  isentropic surface and arrives over Flin Flon on September 15, 0000 GCT. This trajectory has been computed by taking accelerations and decelerations properly

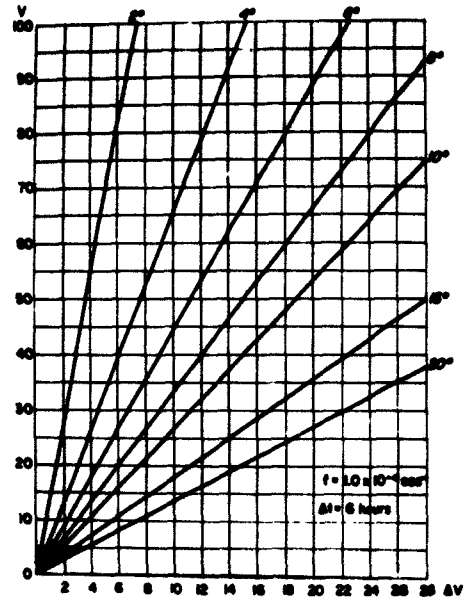


Fig. 9 Evaluation of equation (6) for different angles  $\beta$ ,  $\Delta V$  indicating the 6-hour velocity changes.

into account (Danielsen and Reiter, 1960). Taking

$$\frac{dV}{dt} = -\frac{\partial M}{\partial s} = -\frac{\partial M}{\partial n} \frac{\partial n}{\partial s} \quad (4)$$

where  $s$  indicates differentiation along the trajectory,  $n$  along a normal to the constant-stream function lines of the isentropic surface. Substituting from the geostrophic relationship

$$\frac{\partial M}{\partial n} = -fV \quad (5)$$

we arrive at

$$\frac{dV}{dt} = fV \times \sin \beta \quad (6)$$

where  $\beta$  is the angle between trajectory and constant stream-function lines, indicating the cross-contour flow. Fig. 9 shows an evaluation of equation (6) for  $\Delta t = 6$  hours.

As may be seen from a comparison of Fig. 8 with Fig. 3, the 303°K isentropic trajectory which arrives over Flin Flon on September 15, 00 GCT crosses the jet axis from the cyclonic towards the anticyclonic side near Sachs Harbor shortly before September 13, 12 GCT. By the time the debris particles reach Flin Flon, they have undergone appreciable sinking and are now well to the south of the jet axis.

The sinking motion of the atmospheric layer containing radioactive debris becomes evident from Fig. 10, which shows the soundings of Mould Bay, September 13, 00 GCT and 12 GCT; Sachs Harbor, September 13, 12 GCT; Coppermine, September 14, 00 GCT; and The Pas, September 15, 00 GCT. Unfortunately between Coppermine and The Pas the isentropic trajectory shown in Fig. 8 does not pass in the vicinity of any other upper-air observation. Figs. 11 and 12 contain soundings on either side of the trajectory. The dotted lines in these two diagrams indicate the average soundings between the two stations shown in each figure which, according to Fig. 10, agrees rather well with observations at stations closer to the position of the trajectory.

On September 13, 00 GCT the trajectory comes out of the Arctic region and subsequently passes between Sachs Harbor and Mould Bay. According to Fig. 10, Mould Bay on September 13, 12 GCT lies in the transition zone between cold and warm air, the 303°K stable layer intersecting at 512 mb. The sounding at 00 GCT of this day indicates typical cold-air conditions, as they may have prevailed upstream where the trajectory is found at this map time, with a low tropopause at 320 mb. A stable layer between 320 and 440 mb in this sounding apparently slopes out of the stratosphere and may be indicative of the "jet stream front".

It seems of importance that the stable layer immediately below the tropopause over Mould Bay, September 13, 00 GCT, contains the 303°K isentropic surface at about 390 mb, as does the stable layer over Coppermine, September 14, 00 GCT, at about 612 mb and over The Pas, September 15, 00 GCT at 650 mb. The mechanism of intrusion of stratospheric air into layers of the middle and lower troposphere therefore seems evident. Strongest sinking occurs, while the air particle crosses the jet axis from the cyclonic towards the anticyclonic side, as it does shortly before September 13, 12 GCT somewhere in the vicinity of Mould Bay. During this sinking motion the specific humidity of the air particle should be conserved (Kleinschmidt, 1959; Danielsen and Reiter, 1960). In Fig. 10 maximum possible dew point tempera-

tures have been plotted for significant points reporting "motor-boating" (indicated by "A" in Table II). The actual humidities in these regions may be much

Table II Relative Humidities Reported at Significant Points Enclosing the 303°K Isentropic Surface of Soundings Shown in Fig. 10.

Sounding	Pressure level	Rel. Humidity
Mould Bay 13 Sept., 12 GCT	700	A 15
	<u>529</u> debris	A 18
	510	A 18
Sachs Harbor 13 Sept., 12 GCT	664	A 15
	<u>588</u> debris	A 17
	500	A 18
Coppermine 14 Sept., 00 GCT	<u>794</u> debris	21
	500	A 17
	478	26
The Pas 15 Sept., 00 GCT	<u>662</u> debris	28
	607	A 15

lower than the values plotted in Fig. 10. This fact will help us around the difficulty which is presented by the Mould Bay 1300 sounding: even with saturation at 390 mb over Mould Bay the specific humidity would be much lower than the values plotted at the 303°K surface over the other three stations would indicate. From Table II we may see that the debris carrying 303°K isentropic surface lies in the vicinity of a "motor-boating" report. Conservation of specific humidity could be realized, if the actual humidities were about half of the maximum possible humidities reported with "motor-boating".

According to Reed and Danielsen (1959) the sinking of dry stratospheric air into tropospheric regions occurs in the rather narrow "jet-stream front". This may be demonstrated by means of Fig. 13, in which low relative humidities (< 20%) appearing underneath the North Canadian jet stream (see Fig. 3) may be taken as indicator for such sinking.

From isobaric trajectories one is led to believe that particles traversing the jet axis from the cyclonic to the anticyclonic side would undergo strong accelerations while entering, and strong decelerations while leaving the jet stream. Furthermore, the strong vorticity gradients in the jet axis make a "cross-stream circulation" difficult to understand in view of the theorems of conservation of absolute and potential vorticity.

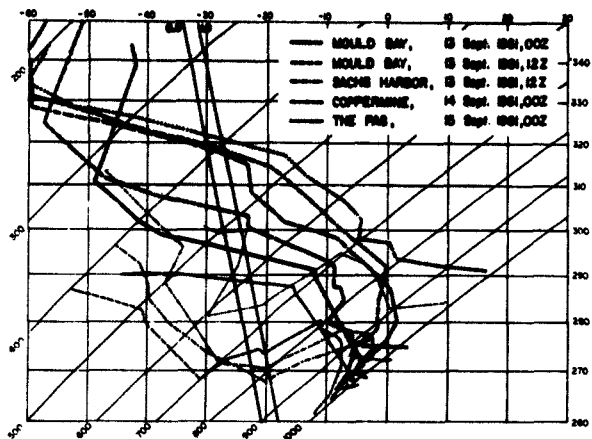


Fig. 10 Temperature and dew point temperature soundings for stations and times as indicated, plotted on a tephigram.

Fig. 11 Temperature and dew point temperature soundings of Fort Smith and Baker Lake, 14 September 1961, 00 GCT. The dotted line indicates the average temperature sounding between the two stations.

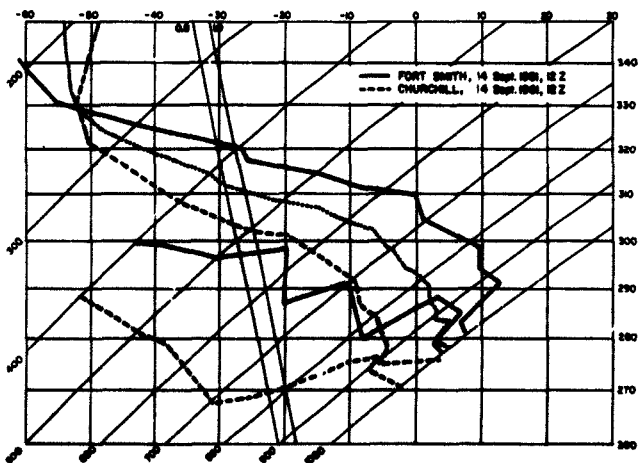
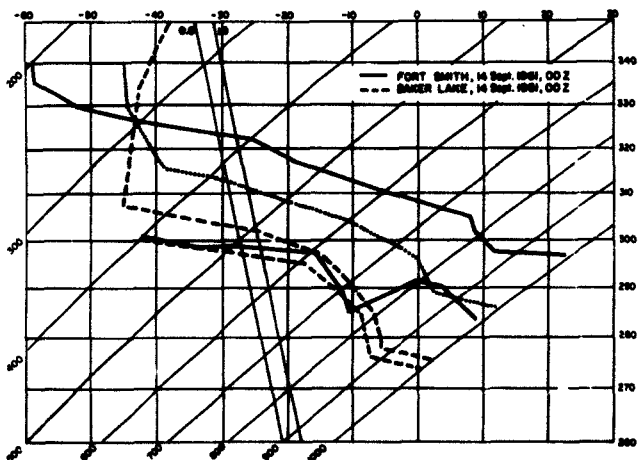


Fig. 12 Temperature and dew point temperature soundings of Fort Smith and Churchill, 14 September 1961, 12 GCT. The dotted line indicates the average temperature sounding between the two stations.

Fig. 13 Montgomery stream-function as in Fig. 7, relative humidities (per cent, areas with <20% irregularly shaded, >80% hatched), and wind speeds (m/sec) and directions (plotted as arrows through station circles) of 303°K isentropic surface.

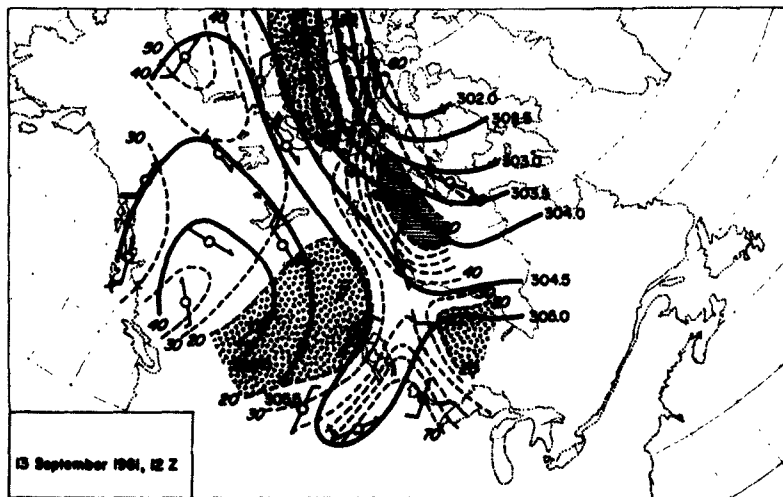
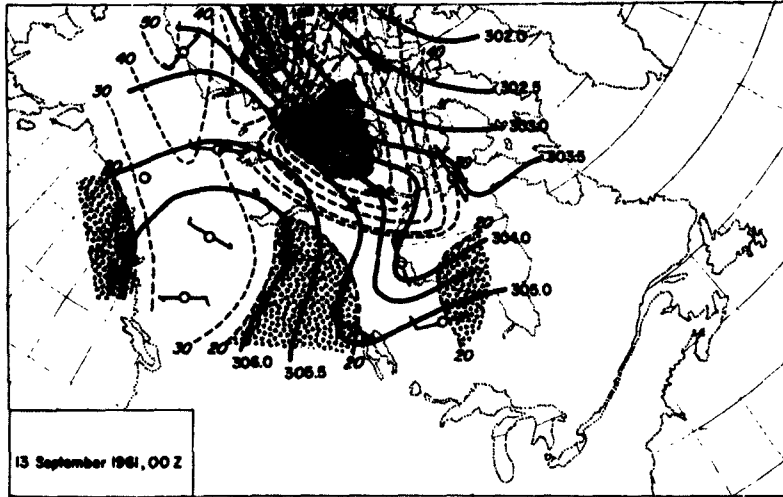


Fig. 13 continued.

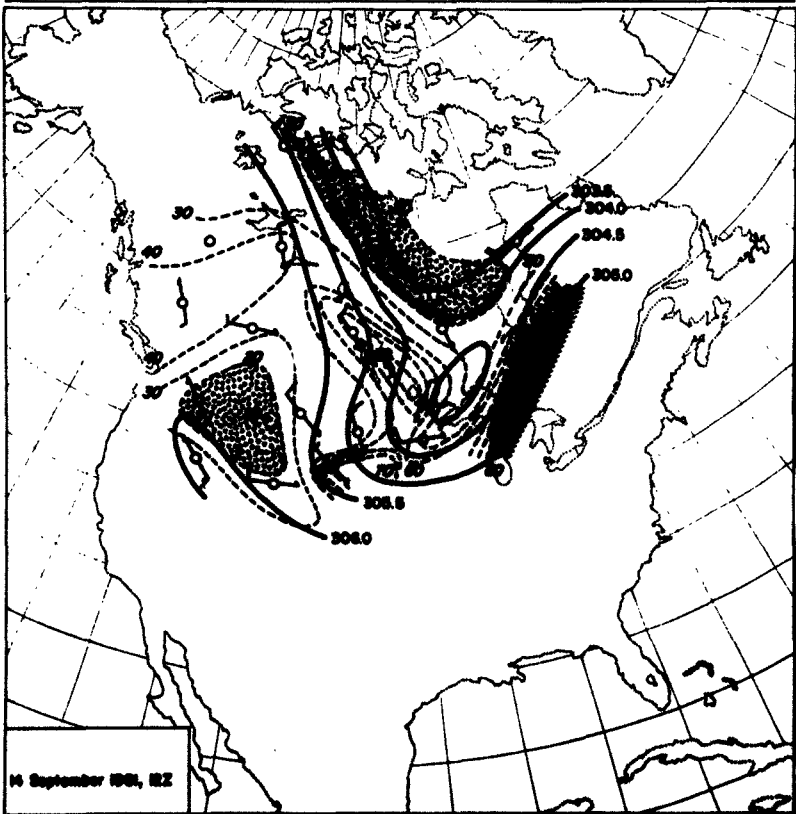
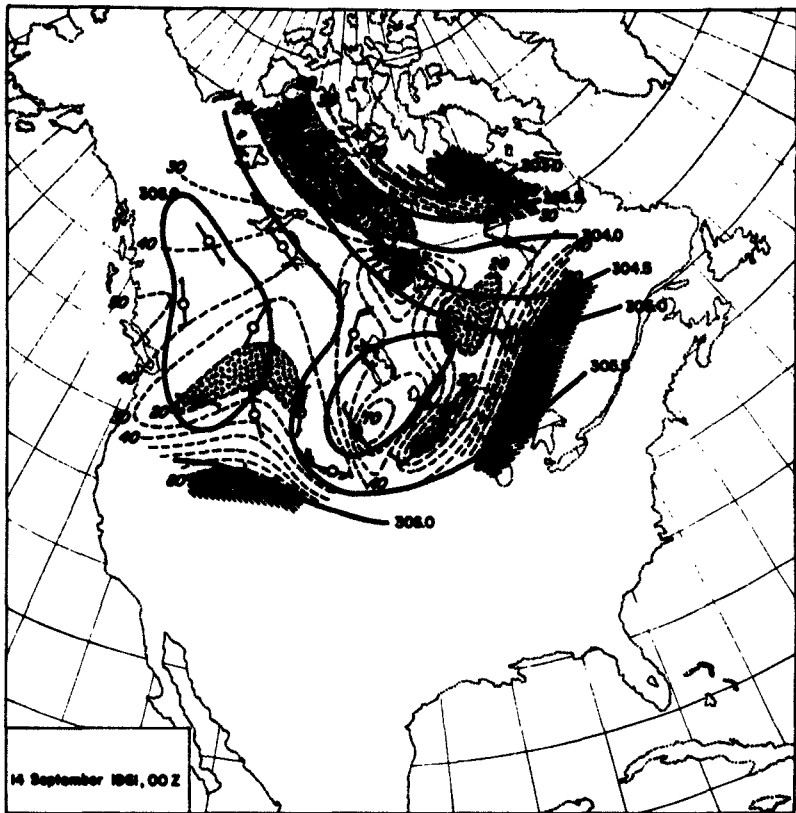
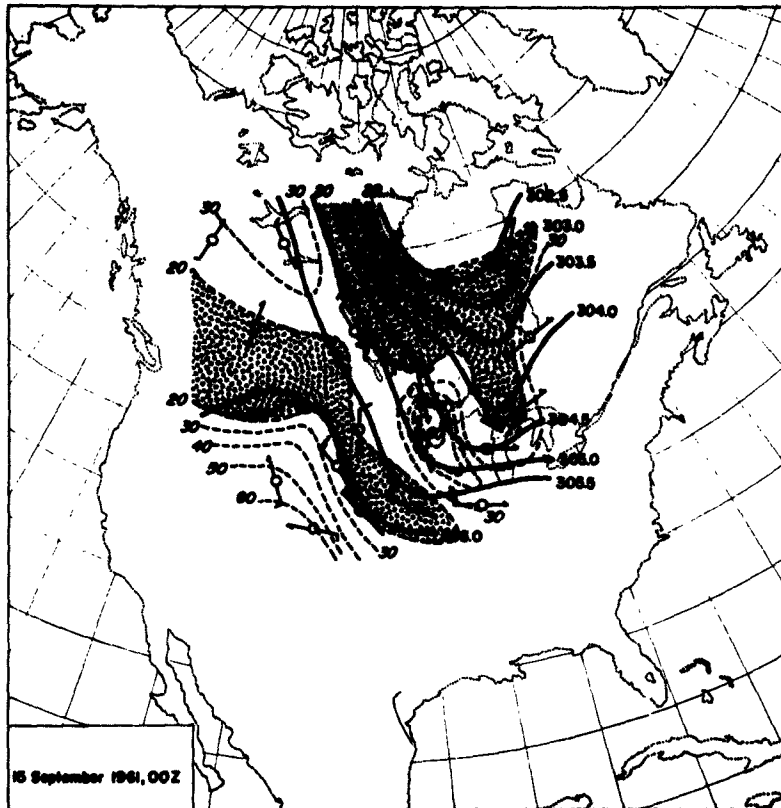


Fig. 13 continued.



As we may see, however, from Figs. 7, 8, and 3 the crossing of the jet axis is associated with almost negligible changes of wind speed along the isentropic trajectory. The main deceleration along this trajectory takes place only after the air particle has reached the influence region of the anticyclone to the south of the jet axis. Fig 14 schematically illustrates this process: The sinking motion --mainly concentrated in the "isentrope trough"\* (Reiter 1960, 1962) and in the "jet-stream front" --carries the air particles along a surface of constant wind speed towards lower layers. The particle thereby more or less maintains its speed and

"crosses" the jet axis by actually "slipping through" underneath the axis. Thus, the potential-vorticity theorem presents no obstacle for this kind of stratospheric-tropospheric mass exchange. This is also evident to some extent from theoretical considerations made by Eliassen (1962).

\*i. e. the downward dip in the isentropic surfaces, usually encountered at jet stream level to the north of the jet axis and evident from a band of relatively warm temperatures on an isobaric surface (see for instance Fig. 3).

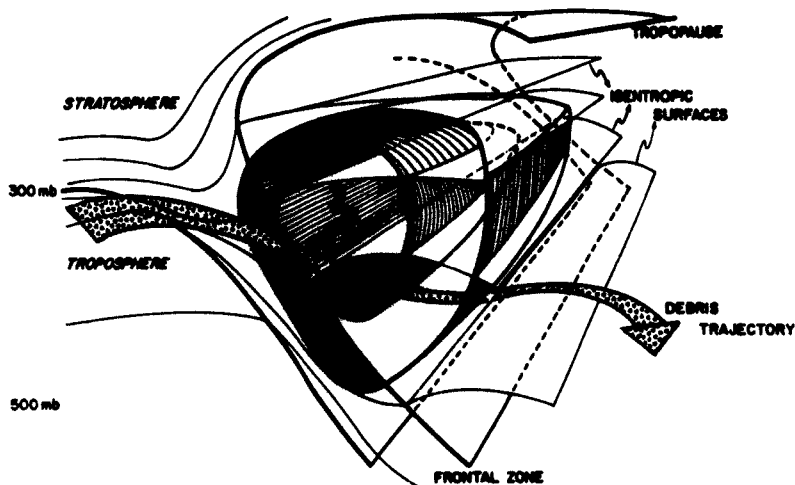


Fig. 14 Schematic trajectory of a debris-carrying air particle (irregularly shaded arrow) in a three-dimensional view of a relative coordinate system which moves with the jet maximum. Isentropic surfaces are indicated by thin lines; surfaces of constant wind velocity, boundaries of the frontal zone and tropopause are marked by heavy lines. The debris in the case outlined here travels at a speed of approximately 60 knots relative to the earth's surface, or ca. 40 knots relative to the moving jet-stream system. By the time the debris reaches the anticyclonic side of the jet stream after strong sinking, it will decelerate. It is still contained within a stable layer which now has the appearance of a subsidence inversion rather than of a strongly baroclinic frontal zone.

THE RADIOACTIVE FALLOUT OVER THE SOUTHEASTERN UNITED STATES,  
SEPTEMBER 17 to 21, 1961

Fig. 15 contains analyses of fallout data from the Public Health Service Radiation Surveillance Network, supplied by the United States Department of Health, Education and Welfare in its monthly tabulation.\* The data are given in  $\mu\text{-Curies per m}^3$  of air. For analysis the results of the laboratory measurements have been used, which are reported in the tabulation mentioned above.

\* The author is indebted to Mr. John Villeforth, United States Public Health Service, for making this data available to him.

As may be seen from this figure, the radioactivity level begins to rise significantly above background values on September 17 over the United States East Coast. On the subsequent days the fallout region spreads to the Gulf Coast and into the mid-western states.

Fig. 16 contains the isentropic stream function, pressures, and winds at the 298°K potential temperature surface. On September 14 these analyses clearly show a small cold dome over the United States-Canadian border region which, by September 15

Fig. 15 Gross beta radioactivity for days indicated, in  $\mu\text{C}$  per  $\text{m}^3$  of particulates in air. Data obtained from laboratory measurements of the Public Health Service Radiation Surveillance Network. Areas with fallout  $>100 \mu\text{C}$  are shaded. Non-linear scale of analysis.

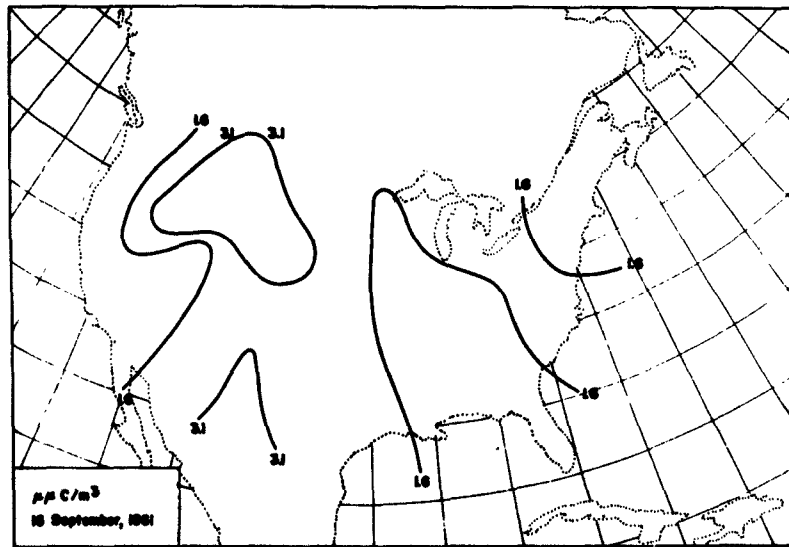
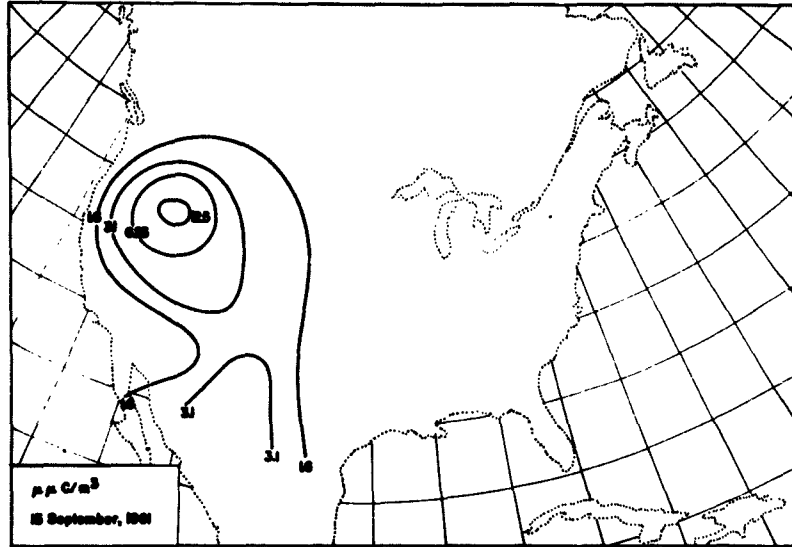


Fig. 15 continued.

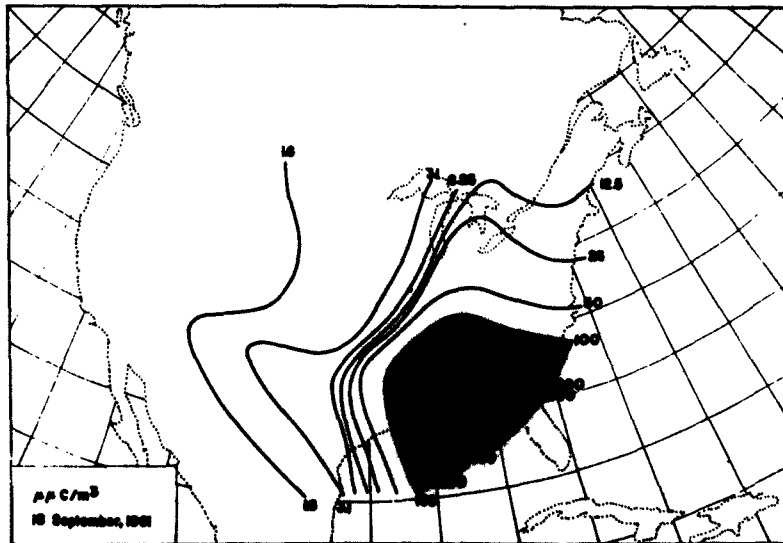
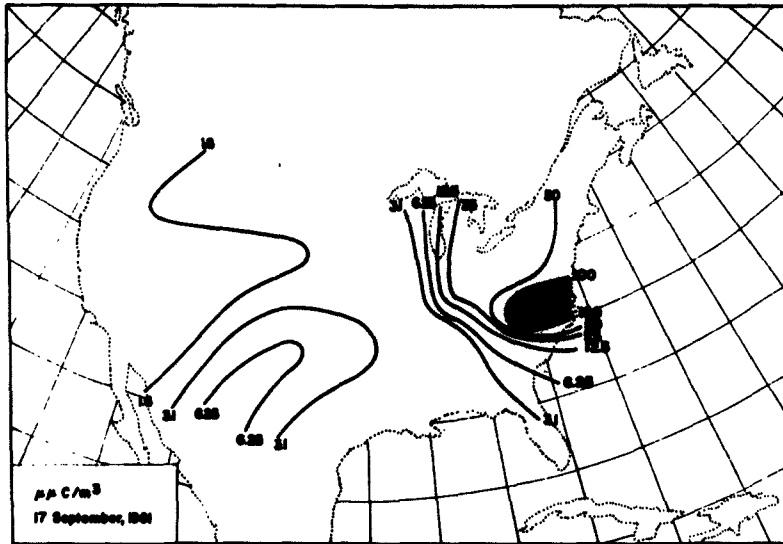


Fig. 15 continued.

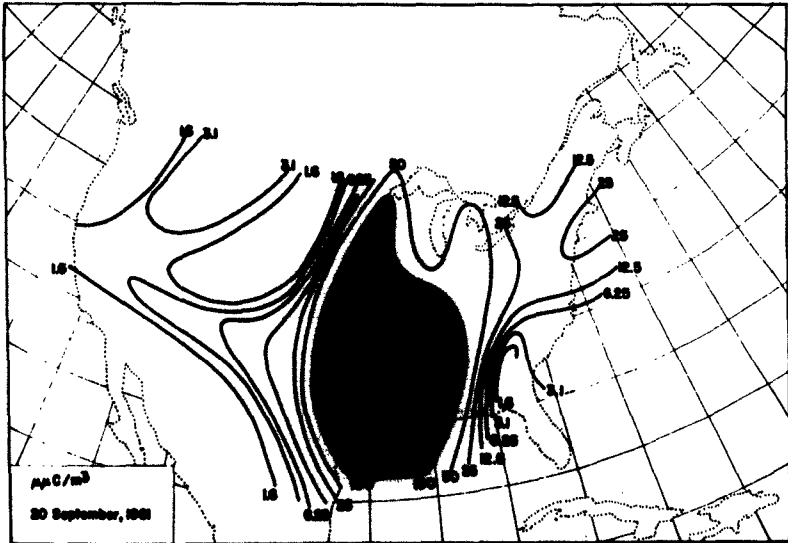
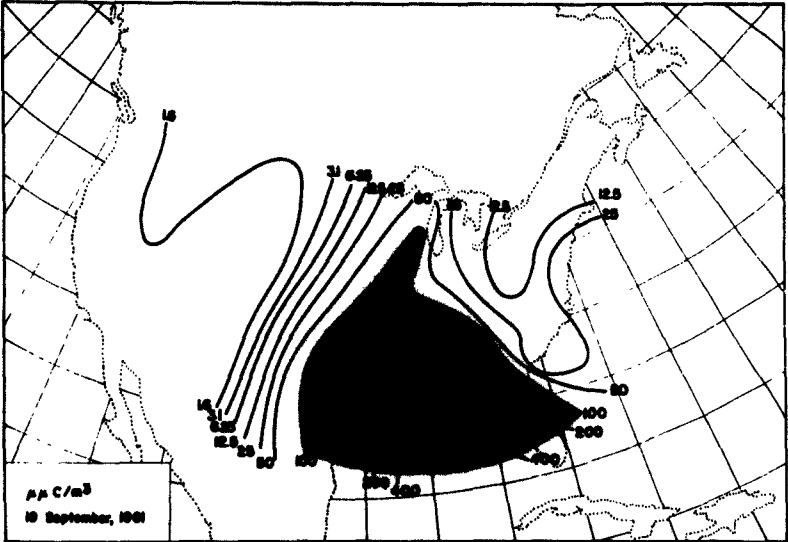




Fig. 16 continued.

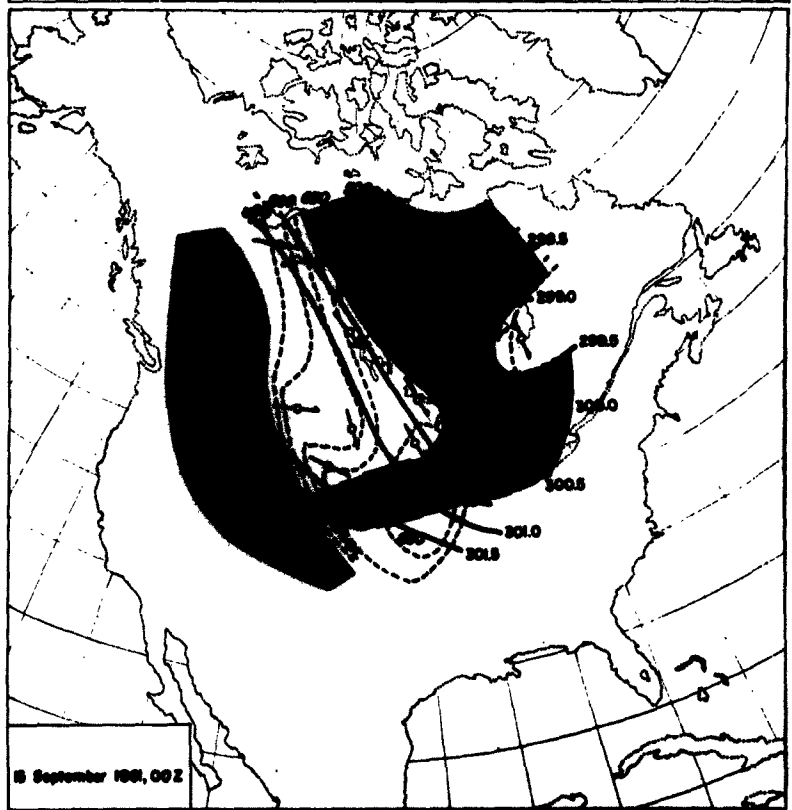
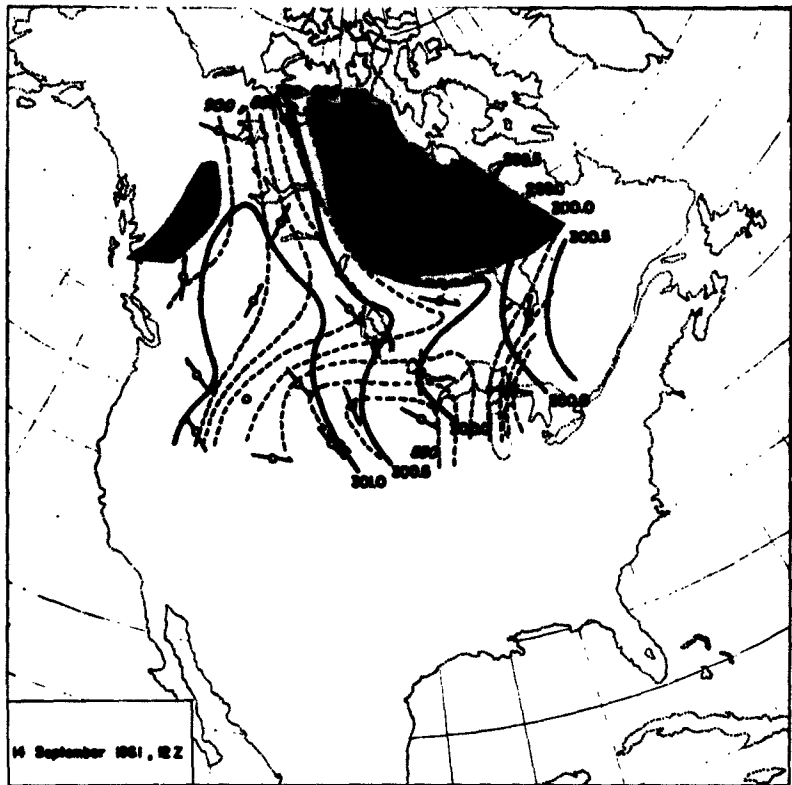


Fig. 16 continued.

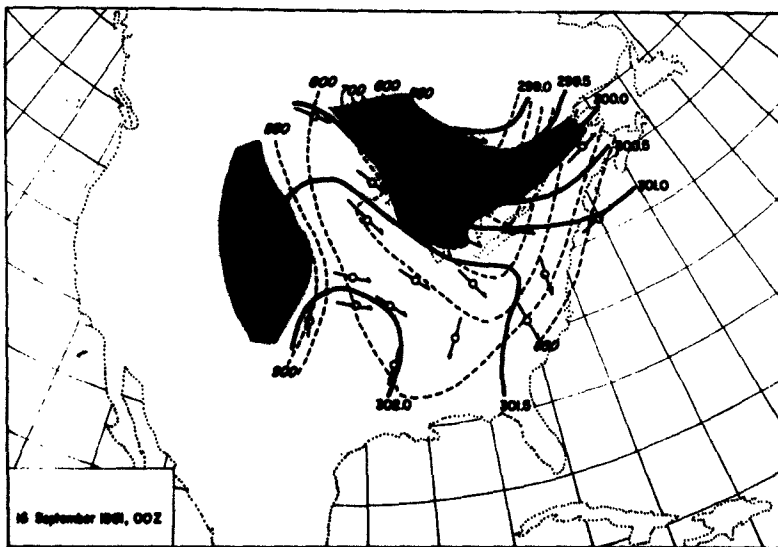
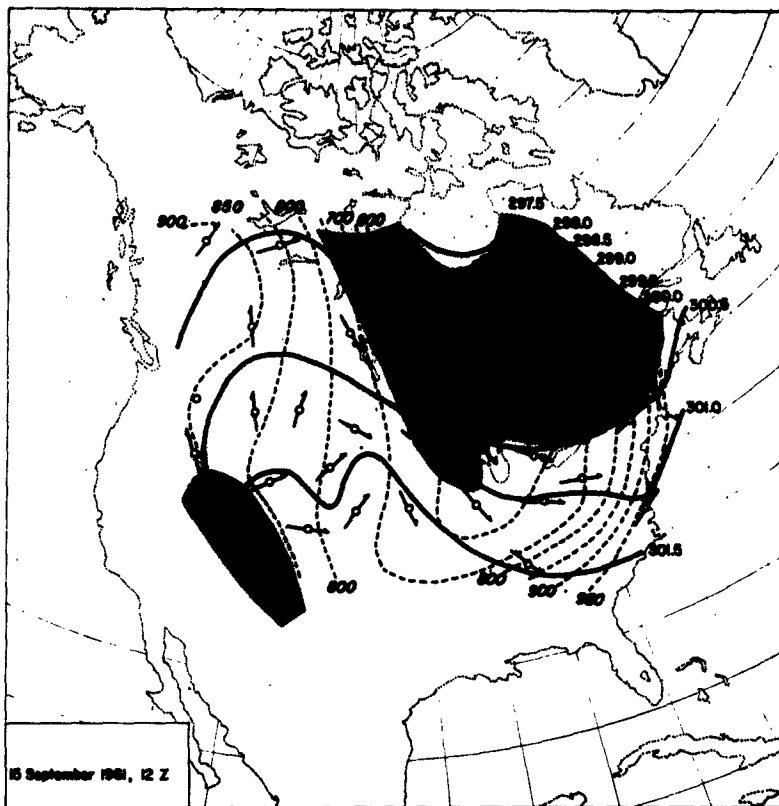
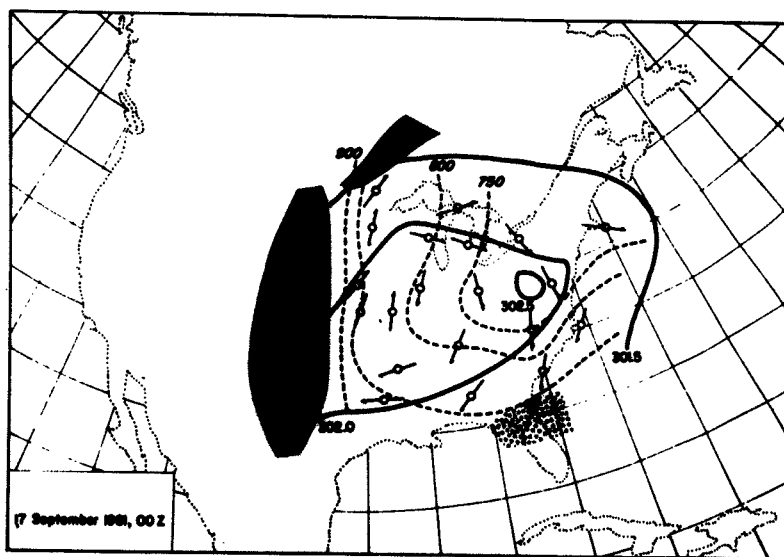
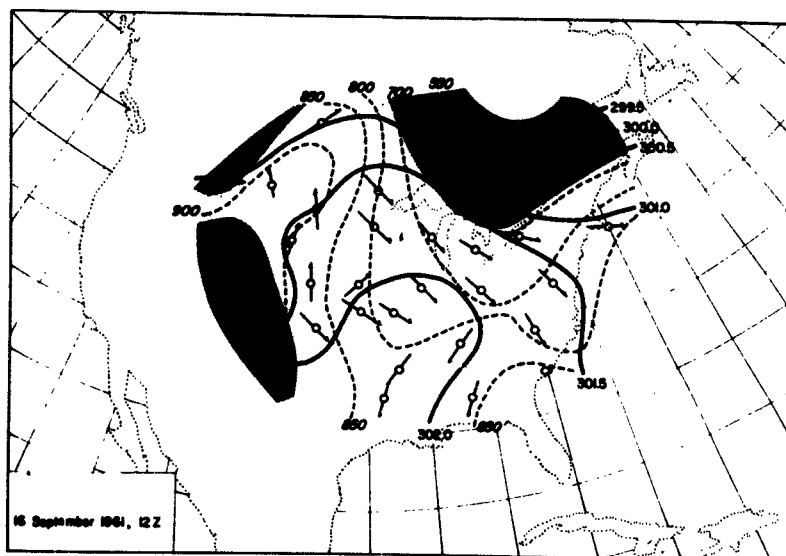


Fig. 16 continued.





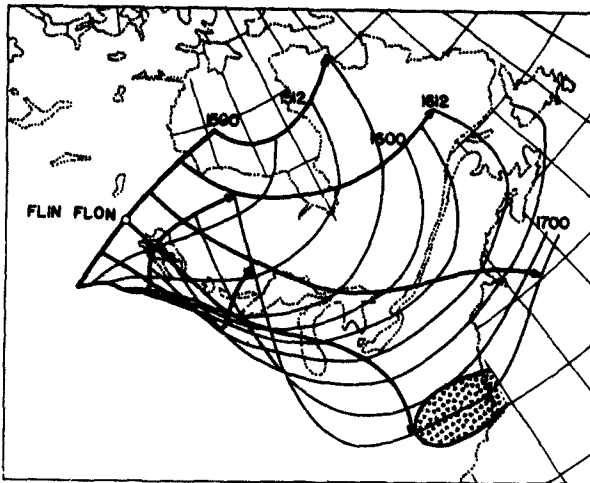


Fig. 17 Trajectories of particles on the 298°K isentropic surface, which were oriented on September 15, 00 GCT along a line through Flin Flon, that intersected the flow at right angles.

collapses. As we will see farther below, this isolated cold air mass is carrying some of the debris which later was deposited over the southern United States.

In Fig. 17 trajectories have been constructed of a line of air particles extending through Flin Flon on September 15, 00 GCT, and oriented approximately normal to the direction of flow at this time. As may be seen from this diagram, the radioactive debris encountered by the Flin Flon ascent arrives over the eastern United States on September 17, when fallout was actually measured there on the ground (Fig. 15). The trajectory of the debris cloud measured over Flin Flon on September 15, 12 GCT bends off towards the northeast. Particles that were located slightly farther to the north, however, also reach the eastern United States (Fig. 18). From Fig. 19 it may be gathered, that the fallout of September 17 over the United States East Coast contained debris which on September 15, 12 GCT was slightly to the east of Flin Flon. As may be seen from the "three-dimensional" view of this trajectory, the air traveling along the 298°K isentropic surface underwent rather marked sinking motion.

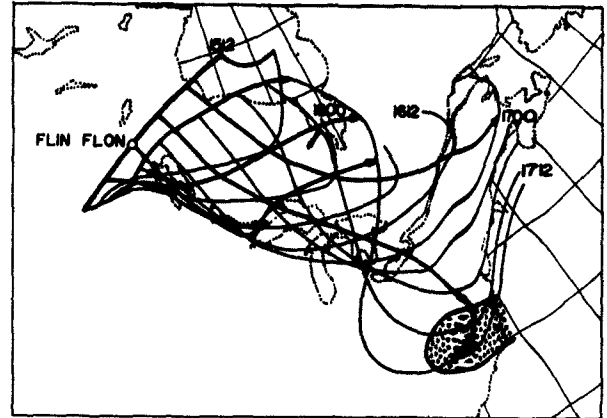


Fig. 18 Same as Fig. 17, except trajectories starting on September 15, 12 GCT.

The isentropic trajectory itself does not reach the ground. It may be assumed, however, that diabatic effects, especially mixing near the ground, and radiative cooling contribute towards the downward transport of debris once the trajectories have reached fairly low levels of the troposphere.

The same holds for Fig. 20, which shows the trajectories of the boundaries of the fallout area of September 18, 12 GCT, over the southern United States. The striking feature of this diagram is, that the fallout in the eastern part of the area traces back to the same area as the fallout of September 17 -- shown in Fig. 19 -- while the debris deposited over the southwestern part of the area stems from the collapsing cold dome shown in Fig. 16. Thus two different sources of debris merge into one fallout area at the ground.

The Public Health Service Tabulation contains an estimate of the approximate age in days of the radioactivity sample. These values are given for several stations in the main fallout area in Table III.

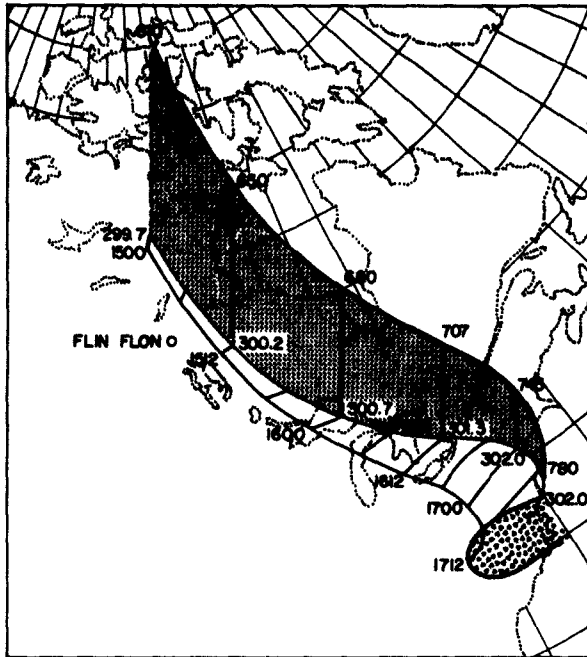


Fig. 19 Trajectories of the boundaries of the fallout area (irregularly shaded) observed on September 17, 1961, 12 GCT over the United States East Coast. The hatched region on top of the northernmost trajectory gives a three-dimensional view of this trajectory: its vertical extent indicates the movement of the particle along the vertical  $p$ -coordinate, the height of the hatched region being proportional to the pressure difference against the 800-mb level; the numbers plotted are pressures (mb), isentropic stream function values ( $10^7 \text{ erg g}^{-1}$ ), and map time of the isentropic surface at these points along the trajectory.

Fig. 20 Same as Fig. 19, only for boundary of fallout region of September 18, 12 GCT. Map times, isentropic stream-function values, and pressures, again, are plotted along the "three-dimensional" and the southernmost trajectories. Marks along the plane trajectories indicate 6-hour displacements.

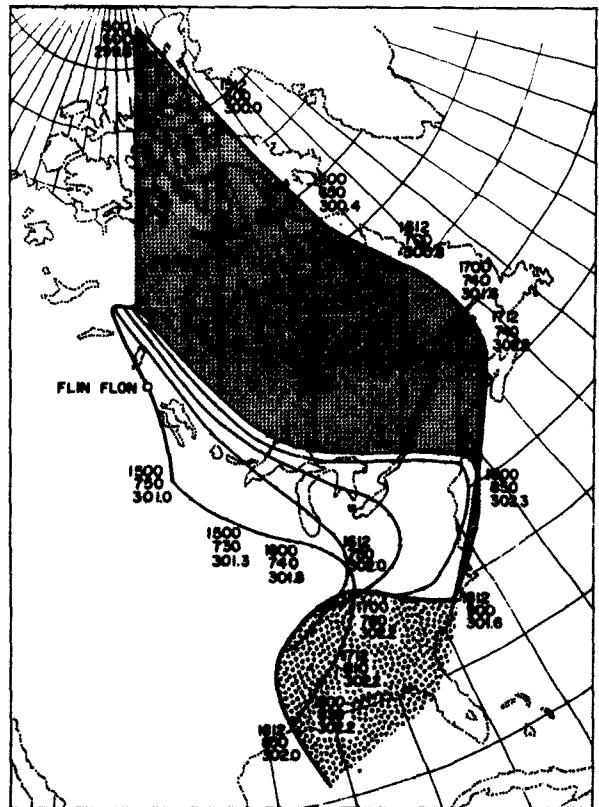


Table III Fallout Data of September 17 to 21, 1961, for Stations in the Main Fallout Regions of Fig. 14

Station	End of Collection		Laboratory Measurement		
	Day	Hour GCT	$\mu\text{C}/\text{m}^3$ gross Beta Radioactivity	Approx. age, days	Estimated date of Nuclear Explosion
Albany, N. Y.	17	12	58.21	7	10
Baltimore, Md.	17	13	58.10	6	11
Gastonia, N. C.	17	13	106.50	6	11
Harrisburg, Pa.	17	14	43.52	11	6
Lawrence, Mass.	17	13	48.04	6	11
Providence, R. I.	17	13	59.91	9	8
Richmond, Va.	17	13	101.94	6	11
Trenton, N. J.	17	16	69.79	7	10
Washington, D. C.	17	18	63.73	6	11
Atlanta, Ga.	18	13	323.60	9	9
Columbia, S. C.	18	14	799.18	5	13
Gastonia, N. C.	18	13	80.39	9	9
Jacksonville, Fla.	18	14	401.16	8	10
Little Rock, Ark.	18	14	101.35	7	11
Nashville, Tenn.	18	14	160.55	9	9
New Orleans, La.	18	18	297.07	8	10
Pascagoula, Miss.	18	14	418.41	10	8
Atlanta, Ga.	19	13	196.08	9	10
Austin, Tex.	19	14	140.00	8	11
Iowa City, Iowa	19	14	105.05	8	11
Jacksonville, Fla.	19	14	113.21	9	10
Jefferson City, Mo.	19	14	194.26	8	11
Madison, Wis.	19	13	123.46	8	11
Nashville, Tenn.	19	14	124.43	8	11
New Orleans, La.	19	15	503.28	8	11
Pascagoula, Miss.	19	14	561.86	9	10
Austin, Tex.	20	14	155.00	11	9
Indianapolis, Ind.	20	14	56.52	11	9
Iowa City, Iowa	20	14	95.46	11	9
Jefferson City, Mo.	20	14	281.43	12	8
Little Rock, Ark.	20	14	708.76	12	8
Lansing, Mich.	20	14	79.47	11	9
Madison, Wis.	20	13	42.07	11	9
Minneapolis, Minn.	20	14	131.58	11	9
Nashville, Tenn.	20	14	119.80	10	10
New Orleans, La.	20	15	143.00	11	9
Oklahoma City, Okla.*	20	20	250.69	12	8
Pascagoula, Miss.	20	14	161.48	10	10
Ponca City, Okla.	20	16	196.12	14	6
Springfield, Ill.	20	14	100.64	11	9
Topeka, Kan.	20	14	302.33	11	9

Table III continued.

Station	End of collection		Laboratory Measurement		
	Day	Hour	$\mu\text{C}/\text{m}^3$ gross Beta Radioactivity	Approx. age, days	Estimated date of Nuclear Explosion
Atlanta, Ga.*	21	13	55.36	13	8
Indianapolis, Ind.	21	14	91.40	15	6
Iowa City, Iowa	21	14	372.94	13	8
Jefferson City, Mo.	21	14	584.35	15	6
Little Rock, Ark.	21	14	283.26	13	8
Madison, Wis.	21	13	210.53	14	7
Minneapolis, Minn.	21	14	385.00	14	7
Nashville, Tenn.	21	14	132.35	14	7
New Orleans, La.	21	17	51.48	15	6
Pascagoula, Miss.	21	14	64.97	13	8
Springfield, Ill.	21	14	286.30	14	7
Topeka, Kan.*	21	14	280.85	15	6

\* indicates precipitation during sampling period.

Table IV Russian Test Series of September 1961. (Anderson, 1962)

Date of Detonation	Site	Approximate Size of Detonation
Sept. 1	S	Substantial Yield, Intermediate Range
4	S	Low Kiloton
5	-	Low to Intermediate Range
6	East of Stalingrad	Low to Intermediate Range
10	NZ	Several Megatons
10	NZ	Low to Intermediate Kilotons
12	NZ	Several Megatons
13	S	Low to Intermediate Yield
13	NZ	Low to Intermediate Yield
14	NZ	Several Megatons
16	NZ	About One Megaton
17	S	Intermediate Yield
18	NZ	About One Megaton
20	NZ	About One Megaton
22	NZ	About One Megaton

All detonations are reported as being "atmospheric".

S - Semipalitinsk

NZ - Novaya Zemlya

According to Tables III and IV the fallout over the eastern United States on September 17 most likely resulted from the Russian tests of September 10. The radioactive debris detected over Flin Flon might have originated from the same tests because it seemed to travel along the same jet stream.

The fallout over the central states which is in part coming out of the collapsing cold dome (Figs. 16 and 20) and which occurs mainly ahead of the advancing cold front (Fig. 2) seems to be intermixed with debris from the nuclear explosion of September 6.

### CONCLUSIONS

The preceding study bears out the following facts:

1. Details of atmospheric meso-structure, as revealed by the existence of thin stable layers, are rather persistent in space and time. This is proven by the shallowness of radioactive debris layers which have traveled over large distances and yet have maintained their identity and their relatively high radioactivity level. Indeed, there seems to be a gap in the spectrum of mixing processes between large-scale synoptic and small-scale turbulent effects, as evident from power spectrum analyses of wind measurements (Van der Hoven, 1957). This gap might help explain the long

life of some meso-structural details in atmospheric stratification.

2. The complexity of atmospheric mixing processes is substantiated by the fact that one and the same high-pressure region near the ground is made up by air masses void of debris, and infested with debris, possibly from two different nuclear blasts.

3. The strong sinking motion associated with a jet stream shortens the residence time of stratospheric air considerably. As pointed out, an isentropic "cross-stream circulation" may be realized which does not conflict with the theorem of conservation of absolute and potential vorticity.

#### ACKNOWLEDGEMENTS

The author is indebted to Drs. K. A. Anderson and E. F. Danielsen for stimulating discussions of the problems presented in this paper. Mr. J. Mahlman performed most of the technical work and computations and Mrs. K. Collins typed the manuscript.

## REFERENCES

- Anderson, K. A., 1962: Thin atmospheric layers of radioactive debris during September 1961. Cosmic Ray Group, Dept. of Physics, Univ. of Calif., Berkeley. Scientific Rept. to ONR. 23 pp.
- Danielsen, E. F., 1959: The laminar structure of the atmosphere and its relation to the concept of a tropopause. Arch. Meteor. Geophys. Biokl. A, 11: 293-332.
- \_\_\_\_\_, 1961: Trajectories: isobaric, isentropic and actual. J. Meteor. 18(4): 479-486.
- \_\_\_\_\_, and E. R. Reiter, 1960: Bemerkungen zu E. Kleinschmidt: Nicht-adiabatische Abkühlung im Bereich des Jet-Stream. Beitr. z. Phys. d. Atmosph. 32(3/4): 265-273.
- Eliassen, A., 1962: On the vertical circulation in frontal zones. Bjerknes Mem. Vol., Geofys. Publ. 24: 147-160.
- Endlich, R. M. and G. S. McLean, 1957: The structure of the jet stream core. J. Meteor. 14: 543-552.
- Hsieh, Y. -P., 1950: On the formation of shear lines in the upper atmosphere. J. Meteor. 7(6): 382-387.
- Kleinschmidt, E., 1959: Nicht-adiabatische Abkühlungen im Bereich des Jet - Stream. Beitr. Phys. d. Atmosph. 32(1/2): 94-108.
- Murgatroyd, R. J., 1959: Jet stream flight of 6 March 1959. Unpublished report.
- Reed, R. J., and E. F. Danielsen, 1959: Fronts in the vicinity of the tropopause. Arch. Meteor. Geophys. Biokl. A, 11: 1-17.
- Reiter, E. R., 1960: The detailed structure of the atmosphere near jet streams. Geofisica Pura e Appl. 46: 193-200.
- \_\_\_\_\_, 1961 a: Meteorologie der Strahlströme (Jet Streams). Springer-Verlag, Vienna, 473 pp.
- \_\_\_\_\_, 1961 b: Die nordamerikanische Strahlstromwetterlage vom 23. bis 27 Januar 1957 an Hand von Forschungsflügen des Project Jet Stream. Beitr. Phys. d. Atmosph. 33(3/4): 244-279.
- \_\_\_\_\_, 1961 c: The detailed structure of the wind field near the jet stream. J. Meteor. 18(1): 9-30.
- \_\_\_\_\_, 1962: Die vertikale Struktur des Strahlstromkernes aus Forschungsflügen des Project Jet Stream. Berichte d. Deutsch. Wetterd. No. 80.
- \_\_\_\_\_, H. Lang, R. Mook, G. Wendler, 1961: Analyse dreier Forschungsflüge des Project Jet Stream. Arch. Meteor. Geophys. Biokl. A, 12: 183-224.

Staley, D. O., 1962: On the mechanism of mass and radioactivity transport from stratosphere to troposphere. *J. Atmosph. Sci.* 19(6): 450-467.

\_\_\_\_\_, 1960: Evaluation of potential-vorticity changes near the tropopause and the related vertical motions, vertical advection of vorticity, and transfer of radioactive debris from stratosphere to troposphere. *J. Meteor.* 17: 591-620.

Van der Hoven, I., 1957: Power spectrum of horizontal wind speed in the frequency range from 0.0007 to 900 cycles per hour. *J. Meteor.* 14: 160-164.